Analytical Biochemistry 509 (2016) 67–72

Contents lists available at ScienceDirect

Analytical Biochemistry

journal homepage: www.elsevier.com/locate/yabio

Characterization of protein expression levels with label-free detected reverse phase protein arrays

Xuexue Guo [a], Yihong Deng [b], Chenggang Zhu [a], Junlong Cai [b], Xiangdong Zhu [c], James P. Landry [c], Fengyun Zheng [d], Xunjia Cheng [b, **], Yiyan Fei [a, *]

[a] Department of Optical Science and Engineering, Shanghai Engineering Research Center for Ultra-Precision Optical Manufacturing, Green Photoelectron Platform, Key Laboratory of Micro and Nano Photonic Structures (Ministry of Education), Fudan University, Shanghai, 200433, China
[b] Department of Medical Microbiology and Parasitology, School of Basic Medical Sciences, Fudan University, Shanghai, 200032, China
[c] Department of Physics, University of California, Davis, CA, 95616, USA
[d] Institutes of Biomedical Science, Fudan University, Shanghai, 200032, China

ARTICLE INFO

Article history:
Received 29 April 2016
Received in revised form
24 June 2016
Accepted 27 June 2016
Available online 29 June 2016

Keywords:
Reverse phase protein arrays
Label-free detection
Quantification
Normalization

ABSTRACT

In reverse-phase protein arrays (RPPA), one immobilizes complex samples (e.g., cellular lysate, tissue lysate or serum etc.) on solid supports and performs parallel reactions of antibodies with immobilized protein targets from the complex samples. In this work, we describe a label-free detection of RPPA that enables quantification of RPPA data and thus facilitates comparison of studies performed on different samples and on different solid supports. We applied this detection platform to characterization of phosphoserine aminotransferase (PSAT) expression levels in *Acanthamoeba* lysates treated with artemether and the results were confirmed by Western blot studies.

1. Introduction

Proteomics is the large-scale study of protein expression levels, post-translational modifications, and functions within biological system to obtain a global, integrated view of disease processes, cellular functions and networks at the protein level [1]. Protein arrays, consisting of thousands or more distinct protein targets immobilized on a solid surface, enable high-throughput analysis of probe-target binding reactions [2] and have been widely used as a promising technology for proteomics [3]. There are generally three types of protein arrays: functional protein arrays, capture protein arrays, and reverse-phase protein arrays (RPPA) [2,4–6]. Functional protein arrays are designed to study biochemistry and functionality of native proteins, peptides or domains and are used for screening molecular interactions, studying protein pathways and analyzing enzymatic activities [7,8]. In capture protein arrays, capture agents such as antibodies are immobilized onto the solid surface and subsequently exposed to a complex sample (such as serum), allowing for simultaneous reactions of the sample with multiple capture agents. They have been used for profiling of protein expression, purification and quantification of antibodies, and detection of biomarkers [9,10]. For RPPA, samples such as cellular lysates, tissue lysates or sera are immobilized on the solid surface [6,11–13] and are then probed with a primary antibody against a specific target protein that may be present in the samples, so that the target protein concentration in the samples may be determined. Advantages of RPPA are that (1) samples do not need to be purified; (2) the target proteins in the samples do not need to be labeled; and (3) only minute amounts of samples are needed for production of the arrays.

Numerous studies have successfully employed RPPA technology in discovery of biomarkers, investigation of signal pathways and evaluation of pharmaceutical targets [14–17]. The RPPA-based assay, first reported by Paweletzin in 2001 [16], is a robust methodology for quantification of protein abundance in cellular samples. Typically cell lysates are spotted on a solid surface and probed with a primary antibody against a specific protein present in the lysates, followed by a biotinylated or fluorescently labeled secondary antibody. The amount of captured secondary antibodies serves as the measure of the expression level for the target protein in the samples. Due to the diversity and the widely varying expression

* Corresponding author.
** Corresponding author.
E-mail address: fyy@fudan.edu.cn (Y. Fei).

http://dx.doi.org/10.1016/j.ab.2016.06.027
0003-2697/

levels of target proteins, RPPA usually incorporates a signal amplification procedure based on catalyzed reporter deposition of substrate with commercially available Catalyzed Signal Amplification (CSA kit) [18]. The target protein concentration is proportional to the amplified signals measured with chromogenic/fluorometric detection systems after data preprocessing [19–21].

Three preprocessing steps, background subtraction, quantification, and normalization, are typically performed to make the data analysis reliable. Various efforts have been made to optimize each step [22]. For background subtraction, the baseline and non-specific signals are subtracted. Spatial variations of sample spot intensities are corrected with control spots on the slide, leading to improvements in inter and intra slide reproducibility [23,24]. For quantification step, background corrected spot intensities are mapped to numbers that linearly estimate the amount of protein in the sample. The amplification based on tyramide catalyzation produces a sigmoidal rather than a linear relationship between spot intensities and target protein concentrations [25]. To obtain robust results and extend dynamic range, every sample is diluted several times to form a dilution series. Various models, linear [16], log-linear [26], logistic [27], and non-parametric [28], have been proposed to convert dilution series into a single value that is indicative of the protein concentration in the sample. For the normalization step, estimated protein expression levels are adjusted to account for sample loading differences and other variations that do not reflect biological differences. Sample loading differences include heterogeneity in cell size and cellular composition. Presently the total protein normalization is obtained through staining proteins with Sypro Ruby, FAST green, or colloidal gold [6]. The ratio of target protein to total protein in each spot on a RPPA represents the relative (not absolute) expression of the target protein in the sample [22,29] and thus RPPA simultaneously measure the relative expression levels of target protein in different samples. However, coefficients of proportionality of the relative expression levels versus true protein concentrations vary from one protein to another due to the difference in affinity of the antibodies to the proteins, making it difficult to directly compare expression levels of different proteins in a sample. In addition, it is also difficult to compare relative protein expressions across laboratories where different staining procedures using different signal scales are employed.

Label-free optical detection of protein concentrations on a solid-supported platform provides a solution to problems associated with fluorescence detection and protein staining in the following ways. By measuring optical signals in response to a layer of protein molecules that have an inherently different refractive index from those of the solid support and the aqueous ambient, the optical methods obtain the information on the protein layer [30,31] without requiring fluorescent labels. Over a suitably large range, label-free optical signals vary linearly with the surface mass density of the protein layer and can thus be calibrated to yield the protein concentration in a complex sample. For example, to determine the expression level of a target protein in a complex sample, one first measures the surface mass density of all the immobilized proteins ("total protein") from the complex sample that is printed on a solid support. Then a primary antibody specifically against the target protein is used to react with the immobilized sample and one measures the surface mass density of the antibodies captured only by the target proteins. In a separate experiment, one measures surface mass densities of immobilized target proteins printed from a dilution series of purified target protein solution on the same solid support and reacts the immobilized target protein with the primary antibody. The purified target protein concentration that yields the same amount of captured primary antibody should essentially be the same as the target protein concentration in the complex sample in the preceding measurement and therefore represents the absolute expression level. The corresponding surface mass density of the captured antibodies in the preceding measurement can then used to as the relative measure of the expression level of the target protein.

Label-free methods can be based on, the polarization state of reflected light [32], interference fringes [33], or a number of other properties [34]. Oblique-incidence reflectivity difference (OI-RD) is a label-free detection technology that is readily compatible with microarray-based assay platform [32,35]. In this paper, we report a study that combines the RPPA platform with the OI-RD detection technology, which enables quantification of RPPA data and facilitates comparative studies performed to samples on different solid supports under various conditions. As an example we studied expression levels of phosphoserine aminotransferase (PSAT) in *Acanthamoeba* treated with artemether. The results correlate well with findings of Western blot studies.

2. Materials and methods

2.1. Purified protein, antibody, cell culture and lysate preparations

Procedures for preparing PSAT recombinant protein (rPSAT) and its monoclonal antibody were described previously [36]. Briefly, the cloned cDNAs of encoding *Acanthamoeba castellanii* PSAT were amplified by PCR. Recognition sites for NdeI and BamHI were added to the forward primer and reverse primer. After digestion, the cDNA fragment was ligated into the pET-19b expression vector, and the constructed plasmid was transformed into *E. coli* BL21 (DE3) pLysS. The expression of His tag fused rPSAT was induced with 0.5 mM isopropyl-β-D-thiogalactopyranoside for 14 h at 20 °C, and the proteins were purified using a QIA express kit (Qiagen, USA). Briefly, *E. coli* cells were harvested and the supernatant was decanted after centrifugation at 10000 g for 10 min. Cells were resuspended in 10 mL ice-cold 1 × Binding Buffer and disrupted by sonication. Cell lysate was then centrifuged to remove the debris at 14000 g for 20 min. The supernatant was added to His Bind Resin, and the bound rPSAT was eluted by Elute Buffer. The eluted protein was dialysed against 1 × phosphate buffered saline (1 × PBS, 10 mM PO_4^{3-}, 137 mM NaCl, 2.7 mM KCl, pH7.4) (Sigma-Aldrich, USA) and analyzed by sodium dodecyl sulphate-polyacrylamide gel electrophoresis (SDS-PAGE) at a 10% gel under reducing conditions.

To prepare the monoclonal antibody, a mixture of 50 μg of rPSAT (1 mg/mL) with 50 μL of Freund's complete adjuvant was injected into the peritoneal cavity of 6-week-old BALB/c mice. rPSAT was then mixed with Freund's incomplete adjuvant for the second immunization after the first injection. Mouse spleen cells were fused with X63Ag8.653 myeloma cells by PEG1500. Hybridoma cells were screened using hypoxanthine–aminopterin–thymidine, hypoxanthine–thymidine and rPSAT before intraperitoneal injection into BALB/c mice to prepare ascites of monoclonal antibody. Specificity of ascites of monoclonal antibody against rPSAT was confirmed by Western blot analysis [36].

Acanthamoeba castellanii was cultured in peptone–yeast–glucose (PYG) medium at 26 °C [37] until the trophozoite reached 90% confluence. *Acanthamoeba* trophozoites were treated with artemether at the concentration of 0.1, 0.15, and 0.2 mg/mL for 12 h. Trophozoites of *Entamoeba histolytica* HM-1:IMSS were axenically cultured in BI-S33 medium [38] supplemented with 10% adult bovine serum at 37 °C, and then harvested in the logarithmic phase of growth.

To prepare lysate, trophozoites of *Acanthamoe bacastellanii* and *Entamoeba histolytica* were harvested by centrifugation at 1500×g for 5 min to remove the culture medium, respectively. The trophozoite pellets were washed three times with 1 × PBS. The

pellets were suspended and disrupted by sonication (80w, 10 times, runs every 2 s) in 1 × PBS. The resultant lysate was centrifuged at 12000×g for 15 min under 4 °C, and the supernatant was collected and quantified using the Bradford method (Bio-Rad, USA).

2.2. Western blot analysis

Acanthamoeba trophozoites were incubated with different artemether concentrations for 12 h. The disrupted and quantified trophozoites (20 μg) from different treatment groups were separated through sodium dodecyl sulphate–polyacrylamide gel electrophoresis. The proteins were transferred from the gel onto a polyvinylidene difluoride membrane, the protein blots were blocked at room temperature with skim milk and then incubated with monoclonal anti-PSAT antibodies overnight at 4 °C, then incubated with HRP goat anti-mouse IgG for 1 h at room temperature. After each incubation step, the membrane was washed with PBS containing 0.05% Tween 20. Proteins were detected using an enhanced HRP-DAB substrate detection kit (TiangenBiotech, China), which consists of 2 mL 1 × HRP reaction buffer, 100 μL 20 × reagent A and 20 × reagent B. The optical density of the bands PSAT in the Western blot analysis was measured by Image J software (NIH, USA). All animal experiments were performed in strict accordance with the guidelines from the Regulations for the Administration of Affairs Concerning Experimental Animal (1988.11.1) and approved by the Institutional Animal Care and Use Committee of Shanghai Medical College, Fudan University, China (Permit Number: 20110320-001).

2.3. Arrays fabrication and processing

Three microarrays were fabricated for different experimental purposes. To study the linearity of the OI-RD technique, we fabricated a microarray consisting of rPSAT printed in duplicate at concentrations of 0.019, 0.038, 0.075, 0.15, and 0.3 mg/mL. Recombinant protein Igl-C and the *Entamoeba histolytica* lysate, both at a concentration of 0.6 mg/mL, were also printed as negative controls. To characterize the protein expression levels in lysate samples, we fabricated the second microarray consisting of the *Acanthamoeba* lysate printed in duplicate at concentrations of 0.0625, 0.125, 0.25, 0.5, and 1 mg/mL. To study variations in level of PSAT in cells treated with artemether, we fabricated the third microarray consisting of four cell lysates, including *Acanthamoeba* lysate and lysates of *Acanthamoeba* trophozoites treated with artemether at the concentrations of 0.1, 0.15, and 0.2 mg/mL, each was printed in triplicate at a concentration of 0.5 mg/mL. Together with the four lysates, rPSAT at a concentration of 0.5 mg/mL was also printed in triplicate. All microarrays were printed on epoxy-functionalized glass slides (CapitalBio Corporation, Beijing, China) using the SmartArrayer136 Microarray Spotter (CapitalBio Corporation, Beijing, China). On each glass slide we fabricated 6 identical microarrays. The average diameter of printed spots is 150 μm and the center-to-center spot separation is 250 μm. The printing chamber was equipped with a humidifier and humidity was set at 60%. The printed slides were stored at 4 °C until further use.

The slide is assembled with a fluidic system and each of the six printed microarrays is housed in a separate chamber. Before reaction, the slide is washed with 1 × PBS *in situ* to remove excess printed materials. The surface is then exposed to 3% skim milk in 1 × PBS for 30 min to block the unprinted region and washed again with 1 × PBS. To determine expression levels of PSAT in lysate samples, the microarray is exposed to a primary antibody at room temperature (dilution, 1:100) for 2 h.

2.4. Imaging RPPA with OI-RD microscope

Immobilized lysate samples and their reactions with primary antibodies were sequentially measured and analyzed with OI-RD scanning microscope at 10 μm step size. The working principle of the OI-RD microscope has been reported previously [39–42]. By using a combination of a photo-elastic modulator (PEM) that alters the light beam from p-polarized to s-polarized, a phase shifter that alters the static phase difference between the polarizations, and an analyzer, the OI-RD microscope measures the difference in fractional reflectivity change between the p-polarized and s-polarized components of the reflected light beam due to the microarray on the glass surface $(r_p - r_{p0})/r_{p0} - (r_s - r_{s0})/r_{s0} \equiv \Delta_p - \Delta_s$. r_{p0} and r_{s0} are reflectivities of the bare glass surface for p-polarized and s-polarized components, respectively; r_p and r_s are corresponding reflectivities of the glass surface covered with immobilized sample layer. When the layer thickness d is much less than the optical wavelength λ, $\mathrm{Im}\{\Delta_p - \Delta_s\}$ is proportional to surface mass density Γ (ng/mm^2) of the layer as follows [43],

$$\mathrm{Im}\{\Delta_p - \Delta_s\} \cong \frac{-4\pi\sqrt{\varepsilon_s}\cos\theta}{(\varepsilon_0 - \varepsilon_s)(\cot^2\theta - \varepsilon_s/\varepsilon_0)} \frac{(\varepsilon_d - \varepsilon_0)(\varepsilon_d - \varepsilon_s)}{\varepsilon_d} \frac{\Gamma}{\rho\lambda} \quad (1)$$

At an incident angle $\theta = 67.5°$ and knowing the glass dielectric constant $\varepsilon_s = 2.31$, the aqueous solution dielectric constant $\varepsilon_0 = 1.77$, the protein layer dielectric constant $\varepsilon_d = 2.03$, and the volume mass density of hydrated protein $\rho = 0.5$ g/cm^3, the surface mass density of the protein layer is related to the optical signal by Ref. [44]:

$$\Gamma = 130 \ \mathrm{ng/mm^2} \cdot \mathrm{Im}\{\Delta_p - \Delta_s\} \quad (2)$$

Using Eq. (2), we convert experimentally measured $\mathrm{Im}\{\Delta_p - \Delta_s\}$ to surface mass density of immobilized targets and subsequently captured proteins for quantitative analysis. The variation in the amount of immobilized targets makes it necessary to measure the surface mass density at all stages of assays. This is practical only with a label-free detection method.

3. Results

Acanthamoeba parasites are causative agents of *Acanthamoeba* keratitis, fatal granulomatous amoebic encephalitis, and cutaneous infections. Deng et al. [45] studied the amoebicidal activity of artemether against *Acanthamoeba castellanii* and found that expression levels of PSAT, a key amino-transferase in the phosphorylated serine biosynthetic pathway of *Acanthamoeba castellanii*, change with concentrations of artemether. Using PSAT in *Acanthamoeba* as a model system, we examined the suitability of the RPPA platform detected with the OI-RD technique for protein expression characterization, specifically issues such as (1) the range of linear relation between the amount of captured primary antibodies and that of the immobilized target rPSAT; (2) the performance of the OI-RD detection method in characterizing the PSAT expression level in a lysate sample printed as a dilution series in RPPA; (3) the performance of RPPA and the OI-RD detection in characterizing protein expression levels of PSAT in four different lysate samples.

3.1. Linearity of the OI-RD detected RPPA assay for protein expression level characterization

We incubated a rPSAT microarray in the solution of a primary antibody for 2 h which was long enough for the reaction to complete.

The microarray consists of purified rPSAT printed at concentrations of 0.019, 0.038, 0.075, 0.15, and 0.3 mg/mL. We measured the surface mass density of the immobilized rPSAT before incubation and the change in surface mass density due to captured antibodies after incubation. Fig. 1(A) shows the image in surface mass density of the as-prepared microarray after excess printed materials were washed off. It is obtained by converting the OI-RD image of the microarray using Eq. (2) into an image of surface mass density Γ. At printed concentrations equal or less than 0.3 mg/mL, Γ for rPSAT increases with the printing concentration. Fig. 1(B) shows the change in surface mass density after reaction of the primary mouse antibody with the microarray. Only rPSAT reacts with the antibody while Igl-C and *Entamoeba histolytica* lysate do not.

Fig. 1(C) displays the amount of captured primary antibodies (in ng/mm^2) as a function of the amount of the immobilized rPSAT (also in ng/mm^2). It clearly shows that the former varies linearly with the latter with a slope of 1.42. Since the molecular weight is 47 kDa for rPSAT [36] and 150 kDa for unlabeled primary antibodies, the factor 1.42 means that on almost every two immobilized rPSAT one primary antibody is captured. This factor depends on the affinity constant, the probe concentration, and the accessibility of the antigen epitope on the immobilized target. Under same assay conditions, this factor is expected to remain a constant. We will later use it and the surface mass density of the captured primary antibodies to deduce the amount of immobilized PSAT printed from cell lysates on a solid surface.

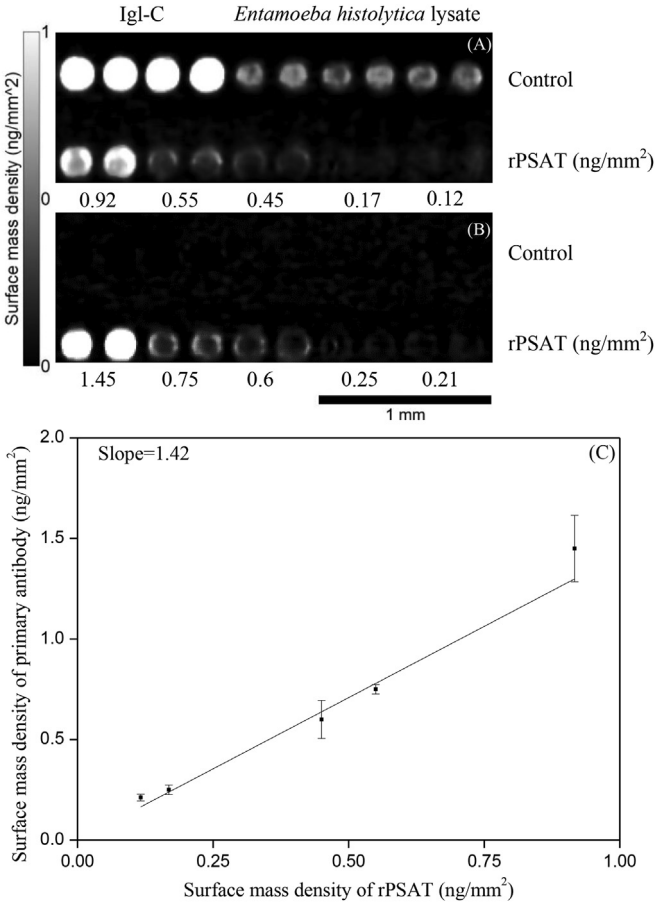

Fig. 1. (A) Surface mass density image of a reverse phase protein microarray printed with pure proteins and cell lysates. (B) Change in surface mass density image of the microarray after reaction with primary mouse antibodies against PSAT. (C) Surface mass density of captured primary mouse antibodies vs. the mass density of the immobilized rPSAT.

3.2. Characterization of PSAT expression levels in Acanthamoeba

We applied the RPPA assay platform to characterization of the PSAT expression level in a *Acanthamoeba* lysate. For this purpose, we incubated an *Acanthamoeba* lysate microarray, printed as a dilution series at lysate concentrations of 0.0625, 0.125, 0.25, 0.5, and 1 mg/mL on the microarray, in the solution of a mouse antibody raised against PSAT. Fig. 2 shows the amount of the captured primary antibodies (in ng/mm^2) vs. that of the immobilized proteins from the lysate. We then extracted the amount of the immobilized PSAT in ng/mm^2 by dividing the amount of the captured primary antibodies by the slope of 1.42 obtained from Fig. 1(C). In doing so we find that 7.7% of the immobilized proteins from the *Acanthamoeba* lysates are PSAT and we will use this number as a measure of the PSAT expression level.

3.3. PSAT expression level in Acanthamoeba treated with artemether

We next applied the RPPA assay platform to determine relative PSAT expression levels in *Acanthamoeba* lysate and *Acanthamoeba* trophozoite lysates treated with artemether at 0.1, 0.15, and 0.2 mg/mL. The RPPA for this study consists of replicates of the four lysate samples printed at a fixed concentration of 0.5 mg/mL. The microarray was incubated in the solution of the mouse antibodies against PSAT for 2 h. From the OI-RD images of the microarray acquired before and after the incubation, we determined the amount of the captured antibodies by the immobilized lysate sample. Following the same procedure in the preceding section, we extracted the amount of immobilized PSAT and its percentage in the total immobilized proteins as the measure of the expression level. The expression level of PSAT in the *Acanthamoeba* lysate without the artemether treatment is 6.4% on this RPPA. The ratio of the immobilized PSAT from a lysate treated with artemether to the immobilized PSAT in the lysate without the artemether treatment can be used as a relative expression level of PSAT in the treated sample. Fig. 3(A) displays the relative PSAT expression levels vs. the artemether treatment. The level of PSAT in *Acanthamoeba* treated with 0.2 mg/mL artemether is reduced to only 18% of the level in the sample without artemether treatment.

Our Western blot analysis [45] also shows that the PSAT expression level in *Acanthamoeba* decreases markedly with treatment of artemether (Fig. 4(B)). The relative changes in optical

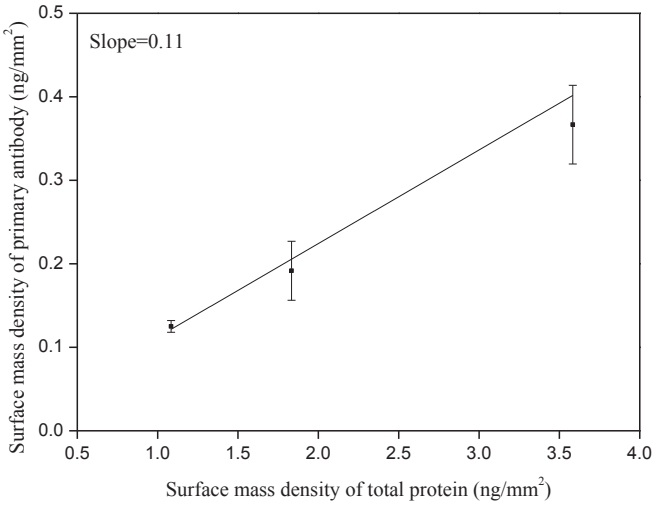

Fig. 2. Surface mass density of captured primary mouse antibodies against PSAT vs. that of the total immobilized proteins from the *Acanthamoeba* lysates.

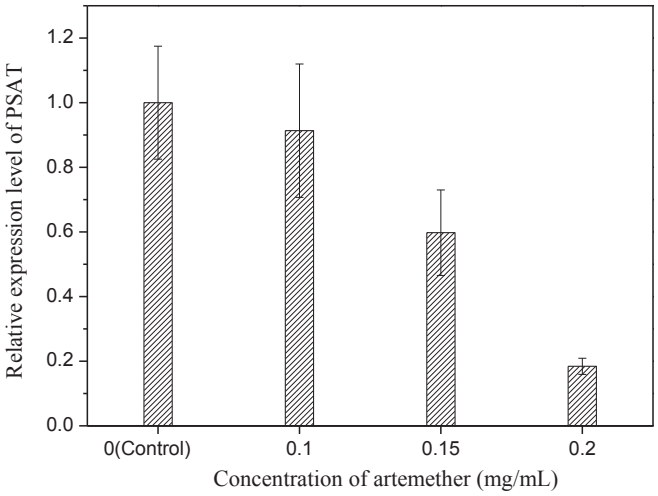

Fig. 3. Relative expression levels of PSAT in artemether-treated *Acanthamoeba* vs. the concentration of artemether from OI-RD detected RPPA assay.

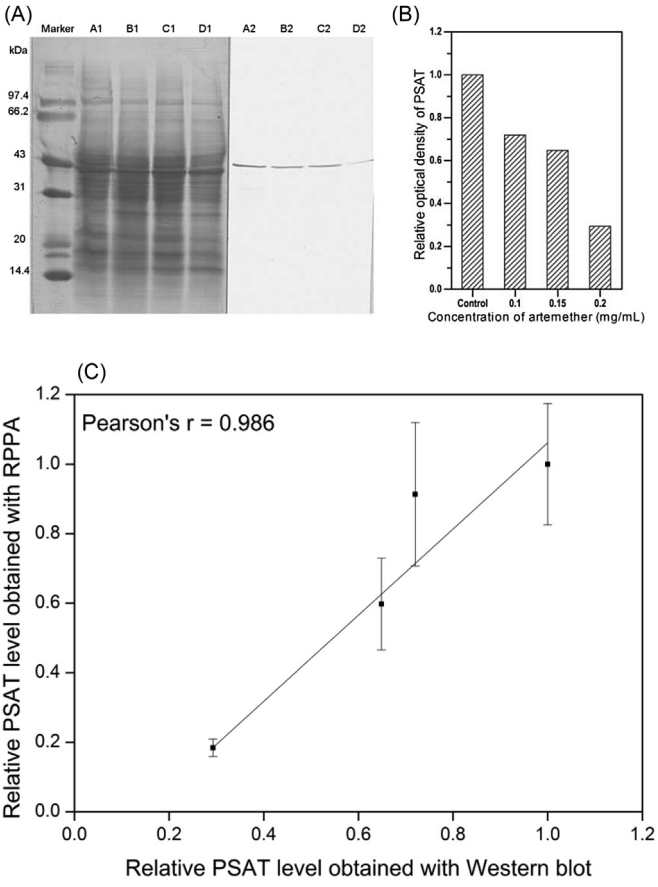

Fig. 4. Down-regulation expression levels of PSAT in *Acanthamoeba* after artemether treatment vs. artemether concentration. (A) Western blot analysis of PSAT from treated *Acanthamoeba* (20 μg total protein extracts). PSAT was detected as a band of 44 kDa. (A1, A2): control, (B1, B2): 0.1 mg/mL, (C1, C2): 0.15 mg/mL, and (D1, D2): 0.2 mg/mL, respectively. (B) Relative PSAT levels in terms of the ratio of the optical density (O.D.) of PSAT in a treated sample to the O.D. of PSAT in an untreated sample. (C) Correlation between relative PSAT levels obtained with the RPPA assay and those obtained with the Western blot analysis.

density of the Western blot analysis show a good correlation ($r = 0.986$) with the relative expression levels obtained with the RPPA assay (Fig. 4(C)).

4. Discussion

Since the introduction of RPPA technology in 2001, it has been implemented in fields ranging from basic science to bio-molecular diagnostics, such as profiling of protein expression, purification and quantification of antibody, and detection of biomarkers. The major advantage of RPPA compared to other techniques analyzing the levels of different proteins (i.e., antibody microarray or mass spectrometry) is that RPPA is able to assess protein levels in large numbers of samples in a cost effective manner with minimum consumption of samples, which is particular important for small amount precious samples available from patients. So far, most RPPA analysis includes chromogenic/fluorometric detection while biosensors based label-free detection of RPPA was less exploited [46], which is expected to act as alternative platforms for confirmation and provide complementary results for large-scale screenings on RPPA.

We presented an assay platform that combines reverse phase protein arrays (RPPA) with label-free detection method OI-RD for protein expression level characterization. The platform allows quantitative determination of surface mass density of immobilized proteins and captured primary antibodies and in turn relative expression levels of target proteins in cell lysates. Compared to chromogenic/fluorometric detected RPPA assays, much simplified procedures of the OI-RD detected RPPA immunoassays minimize errors introduced in staining and amplification processes. By operating in the linear response region, one only needs to perform the RPPA assay of lysate samples at single concentration of a complex sample instead over a dilution series. Since the platform directly determines changes in surface mass density at each step of the assay, one can compare protein expression levels in different samples, on different solid supports, and from different laboratories.

As illustrated in Fig. 3, small changes in protein expression levels can be readily detected on the present platform. The noise level in current OI-RD setup is about 2×10^{-4}, which is equal to detection limit of surface mass density ~26 pg/mm^2. It corresponds to 0.45% of the total immobilized proteins from a lysate sample. By using three-dimensional immobilization substrates (e.g., nitrocellulose or hydrogel coated slides) and Surface-Plasmon-Resonance enhanced OI-RD, the platform has the potential to detect proteins in a cell lysate at concentrations as little as 0.01% by protein mass.

5. Conclusions

We presented a reverse phase protein microarray (RPPA) platform detected by label-free optical detection method OI-RD for quantitative protein expression-level characterization. We illustrated the effectiveness of this platform by investigating the expression level of PSAT in *Acanthamoeba* treated with artemether. The RPPA assay results are in good agreement with the Western blot analysis.

Acknowledgments

This work is supported by the National Natural Science Foundation of China [grant number 61505032]; Scientific Research Foundation for the Returned Overseas Chinese Scholars, Ministry of Education of the People's Republic of China; and the Doctoral Fund of the Ministry of Education of China [grand number 20110071110042].

References

[1] A. Pardanani, E.D. Wieben, T.C. Spelsberg, A. Tefferi, Primer on medical

genomics part IV: expression proteomics, Mayo Clin. Proc. 77 (2002) 1185–1196.
[2] H. Zhu, J.F. Klemic, S. Chang, P. Bertone, A. Casamayor, K.G. Klemic, D. Smith, M. Gerstein, M.A. Reed, M. Snyder, Analysis of yeast protein kinases using protein chips, Nat. Genet. 26 (2000) 283–289.
[3] L. Berrade, A.E. Garcia, J.A. Camarero, Protein microarrays: novel developments and applications, Pharm. Res. 28 (2011) 1480–1499.
[4] O. Poetz, J.M. Schwenk, S. Kramer, D. Stoll, M.F. Templin, T.O. Joos, Protein microarrays: catching the proteome, Mech. Ageing Dev. 126 (2005) 161–170.
[5] M. Janzi, J. Odling, Q. Pan-Hammarstrom, M. Sundberg, J. Lundeberg, M. Uhlen, L. Hammarstrom, P. Nilsson, Serum microarrays for large scale screening of protein levels, Mol. Cell. Proteomics 4 (2005) 1942–1947.
[6] R. Akbani, K.F. Becker, N. Carragher, T. Goldstein, L. de Koning, U. Korf, L. Liotta, G.B. Mills, S.S. Nishizuka, M. Pawlak, E.F. Petricoin, H.B. Pollard, B. Serrels, J.C. Zhu, Realizing the promise of reverse phase protein arrays for clinical, translational, and basic research: a workshop report, Mol. Cell Proteomics 13 (2014) 1625–1643.
[7] H. Zhu, M. Snyder, Protein chip technology, Curr. Opin. Chem. Biol. 7 (2003) 55–63.
[8] J.S. Merkel, G.A. Michaud, M. Salcius, B. Schweitzer, P.F. Predki, Functional protein microarrays: just how functional are they? Curr. Opin. Biotechnol. 16 (2005) 447–452.
[9] S.S. Nishizuka, G.B. Mills, New era of integrated cancer biomarker discovery using reverse-phase protein arrays, Drug Metab. Pharmacokinet. 31 (2016) 35–45.
[10] K. Kume, K. Ishida, M. Ikeda, K. Takemoto, T. Shimura, L. Young, S.S. Nishizuka, Systematic protein level regulation via degradation machinery induced by genotoxic drugs, J. Proteome Res. 15 (2016) 205–215.
[11] A. Silvestri, A. Colombatti, V.S. Calvert, J.H. Deng, E. Mammano, C. Belluco, F. De Marchi, D. Nitti, L.A. Liotta, E.F. Petricoin, M. Pierobon, Protein pathway biomarker analysis of human cancer reveals requirement for upfront cellular-enrichment processing, Lab. Investig. 90 (2010) 787–796.
[12] M. Mazzone, L.M. Selfors, J. Albeck, M. Overholtzer, S. Sale, D.L. Carroll, D. Pandya, Y.L. Lu, G.B. Mills, J.C. Aster, S. Artavanis-Tsakonas, J.S. Brugge, Dose-dependent induction of distinct phenotypic responses to Notch pathway activation in mammary epithelial cells, Proc. Natl. Acad. Sci. U. S. A. 107 (2010) 5012–5017.
[13] C. Mueller, W.D. Zhou, A. VanMeter, M. Heiby, S. Magaki, M.M. Ross, V. Espina, M. Schrag, C. Dickson, L.A. Liotta, W.M. Kirsch, The Heme degradation pathway is a promising serum biomarker source for the early detection of Alzheimer's disease, J. Alzheimers Dis. 19 (2010) 1081–1091.
[14] A. Aguilar-Mahecha, C. Cantin, M. O'Connor-McCourt, A. Nantel, M. Basik, Development of reverse phase protein microarrays for the validation of clusterin, a mid-abundant blood biomarker, Proteome Sci. 7 (2009).
[15] L.M. Moore, K.M. Holmes, S.M. Smith, Y. Wu, E. Tchougounova, L. Uhrbom, R. Sawaya, J.M. Bruner, G.N. Fuller, W. Zhang, IGFBP2 is a candidate biomarker for Ink4a-Arf status and a therapeutic target for high-grade gliomas, Proc. Natl. Acad. Sci. U. S. A. 106 (2009) 16675–16679.
[16] C.P. Paweletz, L. Charboneau, V.E. Bichsel, N.L. Simone, T. Chen, J.W. Gillespie, M.R. Emmert-Buck, M.J. Roth, E.F. Petricoin, L.A. Liotta, Reverse phase protein microarrays which capture disease progression show activation of pro-survival pathways at the cancer invasion front, Oncogene 20 (2001) 1981–1989.
[17] A.G. Sikora, A. Gelbard, M.A. Davies, D. Sano, S. Ekmekcioglu, J. Kwon, Y. Hailemichael, P. Jayaraman, J.N. Myers, E.A. Grimm, W.W. Overwijk, Targeted inhibition of inducible nitric oxide synthase inhibits growth of human melanoma in vivo and synergizes with chemotherapy, Clin. Cancer Res. 16 (2010) 1834–1844.
[18] M.N. Bobrow, T.D. Harris, K.J. Shaughnessy, G.J. Litt, Catalyzed reporter deposition, a novel method of signal amplification – application to immunoassays, J. Immunol. Methods 125 (1989) 279–285.
[19] T. Grote, D.R. Siwak, H.A. Fritsche, C. Joy, G.B. Mills, D. Simeone, D.C. Whitcomb, C.D. Logsdon, Validation of reverse phase protein array for practical screening of potential biomarkers in serum and plasma: accurate detection of CA19-9 levels in pancreatic cancer, Proteomics 8 (2008) 3051–3060.
[20] R. Tibes, Y.H. Qiu, B. Hennessy, M. Andreeff, G.B. Miiis, S.M. Kornblau, Reverse phase protein array: validation of a novel proteomic technology and utility for analysis of primary leukemia specimens and hematopoietic stem cells, Mol. Cancer Ther. 5 (2006) 2512–2521.
[21] L. Dupuy, C. Gauthier, G. Durand, A. Musnier, D. Heitzler, A. Herledan, V. Sakanyan, P. Crepieux, E. Reiter, A highly sensitive near-infrared fluorescent detection method to analyze signalling pathways by reverse-phase protein array, Proteomics 9 (2009) 5446–5454.
[22] E.S. Neeley, S.M. Kornblau, K.R. Coombes, K.A. Baggerly, Variable slope normalization of reverse phase protein arrays, Bioinformatics 25 (2009) 1384–1389.
[23] T. Anderson, J. Wulfkuhle, L. Liotta, R.L. Winslow, E. Petricoin, Improved reproducibility of reverse-phase protein microarrays using array microenvironment normalization, Proteomics 9 (2009) 5562–5566.
[24] P. Kaushik, E.J. Molinelli, M.L. Miller, W.Q. Wang, A. Korkut, W.B. Liu, Z.L. Ju, Y.L. Lu, G. Mills, C. Sander, Spatial normalization of reverse phase protein array data, PLoS One 9 (2014).
[25] M. Sevecka, G. MacBeath, State-based discovery: a multidimensional screen for small-molecule modulators of EGF signaling, Nat. Methods 3 (2006) 825–831.
[26] C. Mircean, I. Shmulevich, D. Cogdell, W.Y. Choi, Y. Jia, I. Tabus, S.R. Hamilton, W. Zhang, Robust estimation of protein expression ratios with lysate microarray technology, Bioinformatics 21 (2005) 1935–1942.
[27] S. Nishizuka, L. Charboneau, L. Young, S. Major, W.C. Reinhold, M. Waltham, H. Kouros-Mehr, K.J. Bussey, J.K. Lee, V. Espina, P.J. Munson, E. Petricoin, L.A. Liotta, J.N. Weinstein, Proteomic profiling of the NCI-60 cancer cell lines using new high-density reverse-phase lysate microarrays, Proc. Natl. Acad. Sci. U. S. A. 100 (2003) 14229–14234.
[28] J. Hu, X. He, K.A. Baggerly, K.R. Coombes, B.T.J. Hennessy, G.B. Mills, Non-parametric quantification of protein lysate arrays, Bioinformatics 23 (2007) 1986–1994.
[29] S. Troncale, A. Barbet, L. Coulibaly, E. Henry, B.L. He, E. Barillot, T. Dubois, P. Hupe, L. de Koning, NormaCurve: a supercurve-based method that simultaneously quantifies and normalizes reverse phase protein array data, PLoS One 7 (2012).
[30] J.M. Brockman, B.P. Nelson, R.M. Corn, Surface plasmon resonance imaging measurements of ultrathin organic films, Annu. Rev. Phys. Chem. 51 (2000) 41–63.
[31] G. Gauglitz, Direct optical detection in bioanalysis: an update, Anal. Bioanal. Chem. 398 (2010) 2363–2372.
[32] C.G. Zhu, X.D. Zhu, J.P. Landry, Z.M. Cui, Q.F. Li, Y.J. Dang, M. Lan, F.Y. Zheng, Y.Y. Fei, Developing an efficient and general strategy for immobilization of small molecules onto microarrays using isocyanate chemistry, Sensors 16 (2016) 378.
[33] E. Ozkumur, J.W. Needham, D.A. Bergstein, R. Gonzalez, M. Cabodi, J.M. Gershoni, B.B. Goldberg, M.S. Unlu, Label-free and dynamic detection of biomolecular interactions for high-throughput microarray applications, Proc. Natl. Acad. Sci. U. S. A. 105 (2008) 7988–7992.
[34] A.K. Sinensky, A.M. Belcher, Label-free and high-resolution protein/DNA nanoarray analysis using Kelvin probe force microscopy, Nat. Nanotechnol. 2 (2007) 653–659.
[35] J.P. Landry, Y.Y. Fei, X.D. Zhu, Y.H. Ke, G.L. Yu, P. Lee, Discovering small molecule ligands of vascular endothelial growth factor that block VEGF-KDR binding using label-free microarray-based assays, Assay Drug Dev. Technol. 11 (2013) 326–332.
[36] Y. Deng, D. Wu, H. Tachibana, X. Cheng, Molecular cloning and expression of phosphoglycerate dehydrogenase and phosphoserine aminotransferase in the serine biosynthetic pathway from Acanthamoeba castellanii, Parasitol. Res. 114 (2015) 1387–1395.
[37] T. Kobayashi, T. Mito, N. Watanabe, T. Suzuki, A. Shiraishi, Y. Ohashi, Use of 5-cyano-2,3-ditolyl-tetrazolium chloride staining as an indicator of biocidal activity in a rapid assay for anti-acanthamoeba agents, J. Clin. Microbiol. 50 (2012) 1606–1612.
[38] L.S. Diamond, D.R. Harlow, C.C. Cunnick, A new medium for the axenic cultivation of Entamoeba histolytica and other Entamoeba, Trans. R. Soc. Trop. Med. Hyg. 72 (1978) 431–432.
[39] Y.Y. Fei, J.P. Landry, Y.S. Sun, X.D. Zhu, J.T. Luo, X.B. Wang, K.S. Lam, A novel high-throughput scanning microscope for label-free detection of protein and small-molecule chemical microarrays, Rev. Sci. Instrum. 79 (2008).
[40] Y.S. Sun, J.P. Landry, Y.Y. Fei, X.D. Zhu, J.T. Luo, X.B. Wang, K.S. Lam, Macromolecular scaffolds for immobilizing small molecule microarrays in label-free detection of protein-ligand interactions on solid support, Anal. Chem. 81 (2009) 5373–5380.
[41] Y.Y. Fei, Y.S. Sun, Y.H. Li, H. Yu, K. Lau, J.P. Landry, Z. Luo, N. Baumgarth, X. Chen, X.D. Zhu, Characterization of receptor binding profiles of Influenza A viruses using an ellipsometry-based label-free glycan microarray assay platform, Biomolecules 5 (2015) 1480–1498.
[42] X.D. Zhu, J.P. Landry, Y.S. Sun, J.P. Gregg, K.S. Lam, X.W. Guo, Oblique-incidence reflectivity difference microscope for label-free high-throughput detection of biochemical reactions in a microarray format, Appl. Opt. 46 (2007) 1890–1895.
[43] J.P. Landry, Y.Y. Fei, X.D. Zhu, Simultaneous measurement of 10,000 protein-ligand affinity constants using microarray-based kinetic constant assays, Assay Drug Dev. Technol. 10 (2012) 250–259.
[44] J.P. Landry, Optical Oblique-incidence Reflectivity Difference Microscopy: Application to Label-free Detection of Reactions in Biomolecular Microarrays, Department of Physics, UC, Davis, 2008. Ph.D Thesis.
[45] Y. Deng, W. Ran, S. Man, X. Li, H. Gao, W. Tang, H. Tachibana, X. Cheng, Artemether exhibits amoebicidal activity against acanthamoeba castellanii through Inhibition of the serine biosynthesis pathway, Antimicrob. Agents Chemother. 59 (2015) 4680–4688.
[46] R. Sjoberg, L. Hammarstrom, P. Nilsson, Biosensor based protein profiling on reverse phase serum microarray, J. Proteomics Bioinform. 5 (2012) 185–189.